J. Fluid Mech. (1984), *vol.* 142, *pp.* 187–200
Printed in Great Britain

Investigating cavity/wake dynamics for a circular cylinder by measuring noise spectra

By S. A. FRY
Department of Mechanical Engineering, University of Southampton, England

(Received 6 June 1983 and in revised form 31 October 1983)

Noise spectra are measured at different distances downstream of a cavitating circular cylinder. The effects of velocity and cavitation number on noise spectra are presented. Together with flow observation the noise measurements allow the cavity development to be described and related to cavity-collapse intensity.

1. Introduction

When a cylinder is immersed in a flowing liquid the liquid has to accelerate around it and a pressure distribution develops around the cylinder. At sufficiently low values of cavitation number σ the liquid will cavitate and the subsequent collapse of these bubbles produces noise and erosion. The cavitation zone grows continually as σ is lowered, but it is known (Ramamurthy & Bhaskaran 1979; Varga & Sebestyen 1972; Selim 1981) that the noise and erosion rate reach peak values at the same value of σ and then decrease as choking conditions are approached. Since noise and damage intensities depend upon the flow conditions downstream of the cylinder the reason for their peak values might be found by investigating cavity/wake dynamics. Cavity lengths and cavity-shedding frequencies have already been measured behind cavitating circular cylinders (Varya & Sebestyen 1966*a*, *b*, 1972; Syamala Rao, Chandrasekhara & Seetharamiah 1972; Chandrasekhara & Syamala Rao 1973; Syamala Rao & Chandrasekhara 1976; Selim 1981), but by themselves they cannot explain why peak values should exist for noise and erosion. To understand this it is first necessary to understand more fully the cavity growth mechanism behind a cavitating cylinder. In this work cavity/wake dynamics are investigated by measuring the spectrum of the noise signal downstream of a cavitating cylinder. Spectrum analysers have been used previously to study the flow behind circular cylinders. Varga & Sebestyen (1966*b*) investigated the relationship between cavity-shedding frequency and cavitation number using a variety of different techniques including a spectrum analyser. This instrument has certain advantages over a stroboscope for frequency measurement since the measured spectrum gives additional information about the physical events. Not only can the predominant shedding frequency be determined by a peak in the spectrum, but it is possible to get an immediate indication of how accurately periodic the shedding is, i.e. a narrow-band spectrum indicates highly periodic shedding, while a broad spectrum indicates more random shedding. Also, the amplitude of the spectrum indicates the intensity of the shedding process. Bearman (1969) used a spectrum analyser to investigate the effect of Reynolds number on vortex shedding from a circular cylinder in air. More recently Mussared (1978) used a spectrum analyser in experiments similar to those of Varga & Sebestyen on cylinders in cavitating flow. In his experiments measurement of cavity-shedding frequencies were taken, but the cavity-shedding process was not discussed. The objective of the present

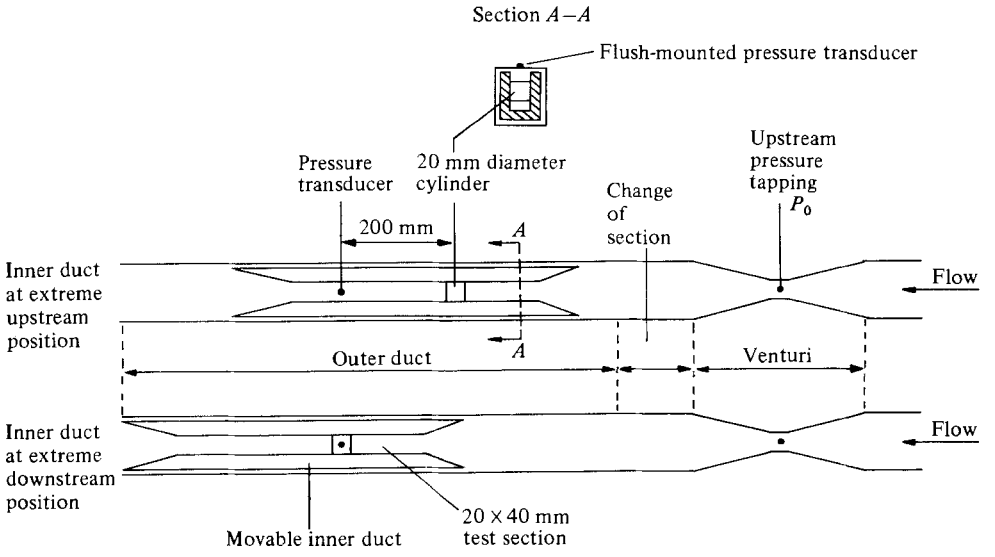

FIGURE 1. Schematic diagram of new test section (plan view). (Reproduced by permission of the Council of the Institution of Mechanical Engineers from Hutton & Fry (1983).)

investigation is to gain a fuller understanding of the cavity development and shedding process as σ is varied, and to relate this process to cavity-collapse intensity.

2. Experimental facility

Experiments were carried out in a closed-circuit water tunnel at the University of Southampton. Water velocity and pressure could be varied independently to give a wide range of flow conditions in the working section. A full description of this tunnel may be found elsewhere (Lobo Guerrero 1974; Lush 1975; Selim 1981).

To allow noise measurement to be taken at different distances downstream of the cylinder a movable duct test section was designed by the author (see figure 1). The pressure transducer remains fixed in the perspex window at the top of the test section while the cylinder can be moved upstream and downstream. It is most important that flow conditions around the cylinder should not be affected by the position of the cylinder. For this reason the cylinder is secured to a movable inner duct so that the boundary-layer growth from the upstream contraction to the cylinder is independent of cylinder position inside the outer duct. Once the desired flow conditions are established the inner duct can be traversed from its extreme upstream position to its extreme downstream position (200 mm) without affecting the cavity dynamics. Further details of this test section may be found in Hutton & Fry (1983).

A considerable amount of experimental work has been carried out by Selim (1981), including extensive weight-loss-rate measurements on both cylindrical and sidewall specimens. To enable the noise measurements from the present investigation to be related to Selim's results the test-section dimensions (20 mm × 40 mm) and cylinder diameter (20 mm) have been kept the same as in his experiments. It is appreciated that this results in a very high blockage (50%), and this is discussed later.

The pressure transducer was of the quartz piezoelectric type made by Kistler (type 603B), which was flush-mounted in a special plastic adaptor to isolate it from

high-frequency accelerations (e.g. noise conducted through the perspex window). The signal from the transducer was amplified by a Vibrometer charge amplifier (type TA-3/C) and then passed to a Hewlett-Packard spectrum analyser (Type 3582A). Signal samples as well as the noise spectrum could be stored and displayed on this instrument. Copies of both were obtained from the spectrum analyser using a Bryans XY recorder (type 26000). Each noise spectrum is an r.m.s. average of 8 noise samples (each of 0.1 s duration). It should be noted that the noise samples were recorded after passing through a low-pass filter which forms an integral part of the spectrum analyser. Accordingly, these samples may not be used for an accurate determination of the cavity collapse signature, but are included here to give an indication of the nature of the collapses. In some of the experiments the amplified signal was passed to a digital r.m.s. voltmeter which has internal filters so that the r.m.s. voltage of the signal is measured in the 50 Hz–50 kHz frequency range. The signal was also monitored on an oscilloscope.

The perspex window allowed the trailing cavities to be observed throughout all experiments. Measurements of shedding frequency were obtained using a Dawe stroboscope (type 1222A), while average cavity lengths were measured directly by eye without using stroboscopic light.

3. Experimental procedure

3.1. *Effect of transducer position on noise spectrum (peak noise conditions)*

The inner duct was set in the upstream position so that the pressure transducer was 200 mm downstream of the cylinder. Peak noise conditions were established by varying the tunnel pressure at a fixed upstream velocity of 19 m/s. It was a simple matter to identify peak noise (maximum r.m.s. voltage of noise signal), since it was found to coincide with peak noise perceived in the laboratory. Peak noise can be identified readily in figure 6, discussed later in the paper. Maintaining these conditions the inner duct was traversed and the noise spectrum (together with noise samples) measured at a number of positions along the duct until the cylinder was situated directly beneath the pressure transducer.

3.2. *Effect of velocity on noise spectrum (peak noise conditions)*

Peak noise conditions were established at different velocities with the pressure transducer 200 mm downstream of the cylinder. The noise spectrum was measured and noise samples recorded at each velocity. Measurements of cavity-shedding frequency were also obtained by arresting the apparent motion with a stroboscope.

3.3. *Effect of cavitation number on flow conditions and noise measurements*

In these tests the inner duct remained fixed with the pressure transducer 200 mm downstream of the cylinder while the cavitation number was varied. The tunnel velocity was held constant at $U_\infty = 16$ m/s and the tunnel pressure varied to cover the full range of cavitating conditions from non-cavitating flow to choked flow. Flow observations were recorded while cavity lengths and r.m.s. pressures were measured. Afterwards measurements of noise spectrum were taken at different values of σ at $U_\infty = 19$ m/s.

4. Results

All tests were carried out using tap water at ambient temperature. The tunnel was run under intense cavitating conditions and any air from water bled off to achieve equilibrium air content before each test.

Results are presented in terms of the cavitation number σ based on flow conditions in the 20 mm × 40 mm test section upstream of the cylinder.

It is well known (Varga & Sebestyen 1966*a*, *b*; Syamala Rao *et al.* 1972; Chandrasekhara & Syamala Rao 1973; Syamala Rao & Chandrasekhara 1976; Selim 1981) that in the early stages of cavitation the cavities downstream of the cylinder are unsteady and cyclic in nature. Such an unsteady cavity flow cannot have a true cavity length, but the naked eye sees a time average of events and the cavitation cloud behind the cylinder looks like a short cavity. Accordingly cavity length was taken as the distance from the cylinder centreline to the position where the cavity was judged by eye to be ending. Further discussion on the erosion patterns and downstream noise distribution resulting from both cyclic and fixed (steady) cavities may be found in Hutton & Fry (1983).

It should be noted that in this investigation a narrow-band spectrum analyser is used only as a tool to give information about the cavity collapse frequency, which may lead to an improved understanding of the cavity-development process. It is not intended to provide quantitative noise-level measurements inside the duct. Such measurements are complicated by a number of factors, including noise attenuation by bubbles in the flow, noise absorption by the walls and possible duct resonances. Considering the test section as a duct, the cut-off frequency will be 18.7 kHz based on the test-section width. While the highest frequency shown in the figures is 2.5 kHz, it is difficult to assume that there is no attenuation in the noise measurements below this cut-off frequency. This is because one of the tunnel walls is perspex and the interface of the water–perspex will constitute a compliant rather than rigid duct boundary. An accurate assessment of this interface influence and other factors is difficult. However, in the present discussion we are concerned with the cavity-collapse frequency, which can be obtained from the noise-spectra measurements.

4.1. *Noise spectra at different positions along duct (at peak noise)*

Peak noise conditions were established as outlined in §3.1. Peak noise was found to occur at $\sigma \approx 4$ with a cavity length of approximately 40 mm. The distance x of the pressure transducer downstream from the cylinder was measured between their centrelines. Figure 2 shows noise spectra measured at different distances downstream of the cylinder. The noise spectrum at $x = 200$ mm has a marked peak at 744 Hz, showing that at that position the pressure transducer was picking up pressure pulsations from the two rows of shed cavities (one from either side of the cylinder) equally. Stroboscopic measurements confirmed that this was the frequency $2f$ of cavities from both sides of the cylinder (f is the cavity-shedding frequency).

With the pressure transducer nearer the cylinder at $x = 90$ mm the energy is increased at the frequency $2f$ because the transducer is closer to the collapsing bubbles. However, it can be seen that there is now also a narrow-band peak in the spectrum at f, suggesting that the transducer is beginning to pick up more signal from the cavities collapsing from one side of the cylinder than from the other. This seems reasonable since the transducer is situated at the top of the duct while the cylinder spans the duct. The transducer is therefore closer to one side than the other. When the transducer was further downstream at $x = 200$ the amplitude of the pressure

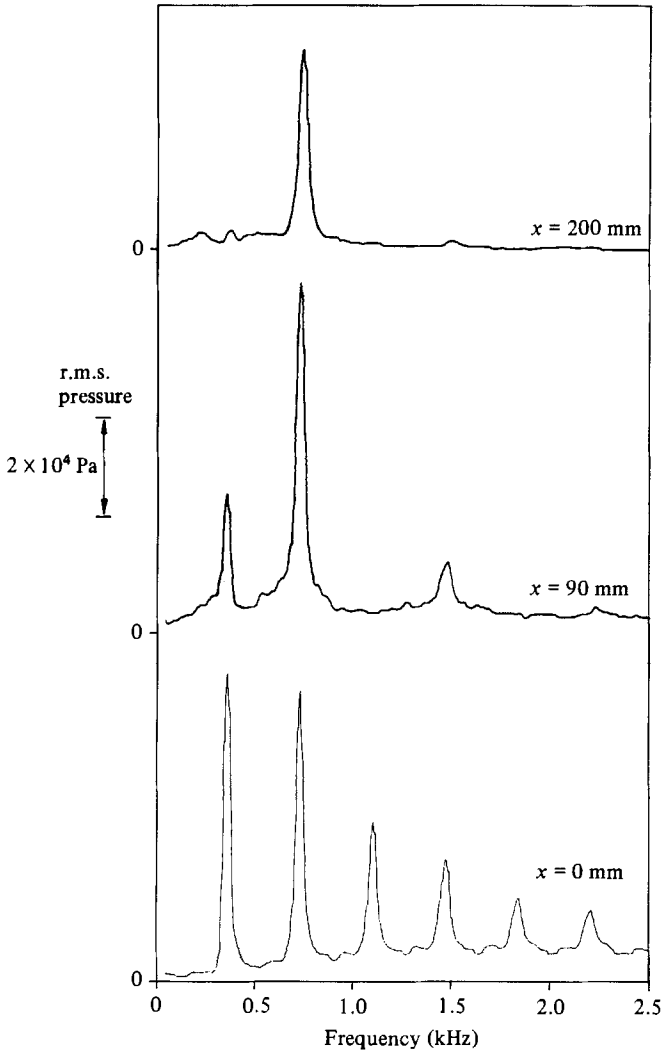

FIGURE 2. Noise spectra at different distances downstream of cavitating cylinder; $\sigma = 4$, $U_\infty = 19$ m/s.

pulsations from the two rows were nearly the same. It should also be noted that a third peak has appeared at a harmonic of f.

When the pressure transducer is located directly above the cylinder at $x = 0$ mm the measured noise spectrum appears more complicated. Here it can be seen that the energy at $2f$ has decreased while the energy at f has increased considerably, i.e. the transducer is sensing a much stronger signal from the collapses in the upper row than those in the lower row. Not only are the cavity collapses in the lower row further from the transducer, but the noise from these collapses may be shielded to some extent by the bubbles in the upper row. It should also be noted that energy peaks have appeared at a number of harmonics of f.

The noise spectra shown in figure 2 should be compared with the noise samples recorded at each transducer position (see figure 3). 200 mm downstream of the cylinder the noise signal shows pulsations corresponding to collapses in both rows. The signal

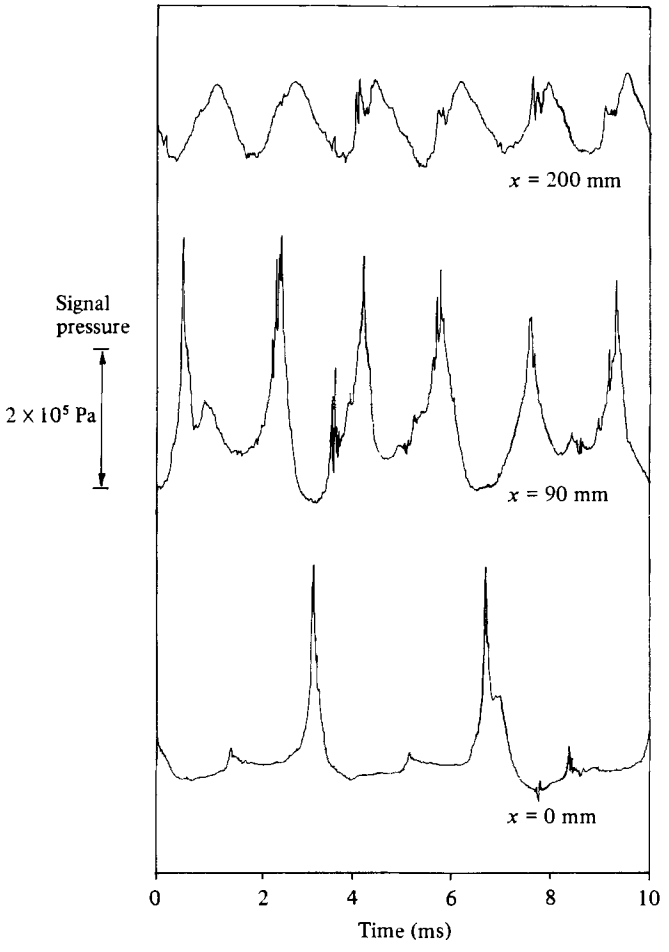

FIGURE 3. Low-pass filtered time function at different distances downstream of cavitating cylinder; $\sigma = 4$, $U_\infty = 15$ m/s.

appears well rounded due to increased attenuation at the higher frequencies. At $x = 90$ mm the attenuation is less and the signal has spikes. Directly over the cylinder the signal shows marked spikes at half the frequency of the two previous signals, i.e. the signal is predominantly from the collapses in the upper row of cavities.

Since the noise spectrum is more simply interpreted at $x = 200$ mm the transducer was located at this position for the remainder of the experiments reported in this paper.

4.2. *Noise spectra at different velocities (at peak noise)*

Figure 4 shows the noise spectra measured at three values of upstream velocity under peak noise flow conditions ($\sigma = 4$). It can be seen that increasing velocity increases the frequency $2f$ at which cavities are shed from both sides of the cylinder and also increases the energy at this frequency. Cavity collapses not only become more frequent with an increase in velocity, but their intensity is also increased. These effects can be seen in the corresponding noise samples shown in figure 5.

Measurements of cavity-shedding frequency were also made using a stroboscope

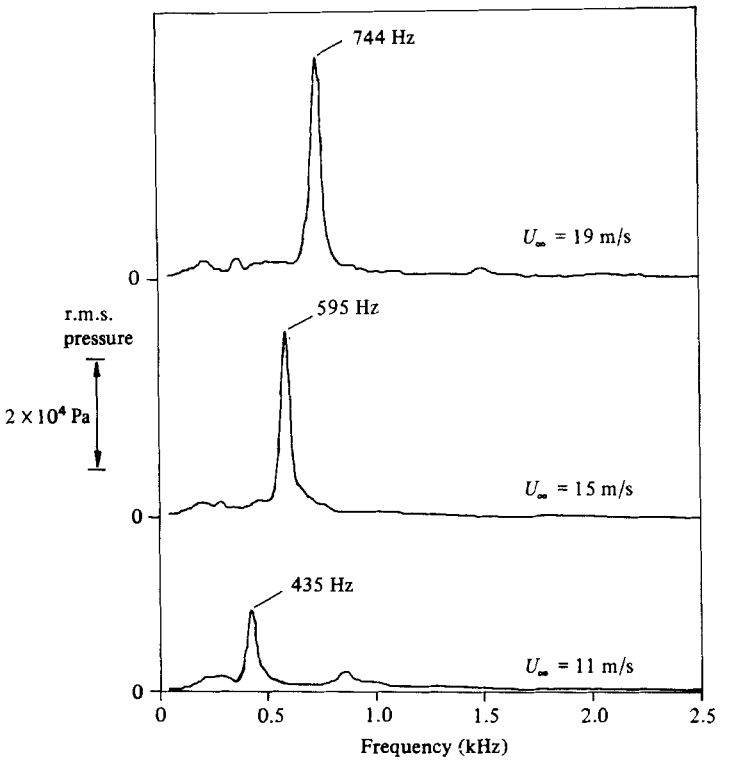

FIGURE 4. Noise spectra at different velocities; $\sigma = 4$, $x = 200$ mm. Peak frequencies measured using digital marker on spectrum analyser display.

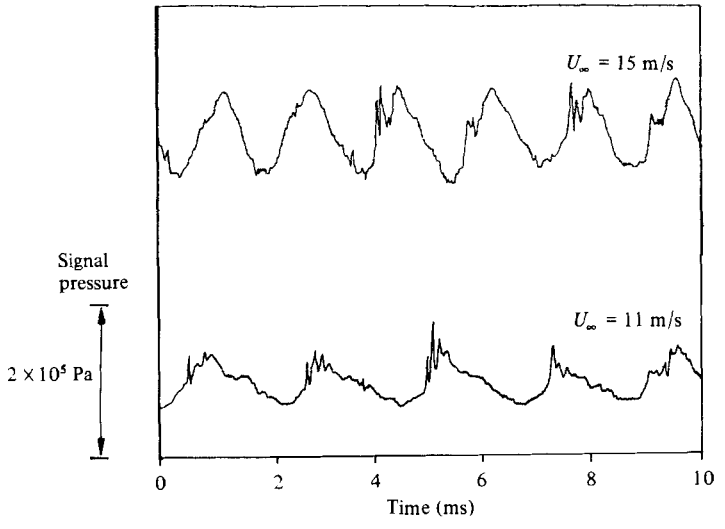

FIGURE 5. Low-pass filtered time function at different velocities; $\sigma = 4$, $x = 200$ mm.

U_∞ (m/s)	Apparent cavity length (mm)	Frequency of peak in noise spectrum (Hz)	Frequency of cavities shed from both sides of cylinder ($= 2f$) using stroboscope (Hz)	$S = \frac{fd}{U_\infty}$
19	40	744	743	0.39
15	40	595	593	0.40
11	40	435	433	0.39

TABLE 1. Comparison between peak frequency in noise spectrum and the frequency $2f$ of cavities shed from both sides of cylinder from stroboscopic measurements; $\sigma = 4$, $x = 200$ mm

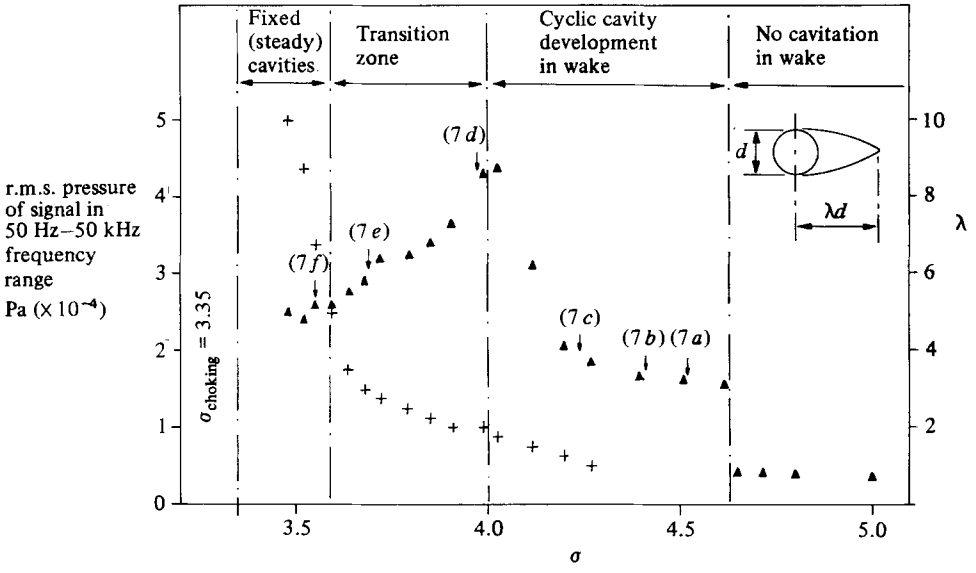

FIGURE 6. Root-mean-square noise (▲) and non-dimensional cavity length (+) *vs.* cavitation number; $U_\infty = 16$ m/s, $x = 200$ mm. Numbers in brackets refer to the noise spectral curves (*a–f*) in figure 7.

and these results are compared with peak frequency values from the noise spectra in table 1. Results obtained from spectral analysis are in good agreement with the frequencies determined by the stroboscope. It can also be seen that the measured cavity-shedding frequencies gave the same values of Strouhal number at each velocity.

As expected the cavity length remained constant (at 40 mm) at peak noise flow conditions independent of velocity.

4.3. *Flow conditions and noise measurements at different values of cavitation number*

The cavitation number was varied as described in §3.3 while the tunnel velocity was held constant. The noise signal 200 mm downstream of the cylinder was passed to the digital r.m.s. voltmeter and cavity lengths were measured by eye. Figure 6

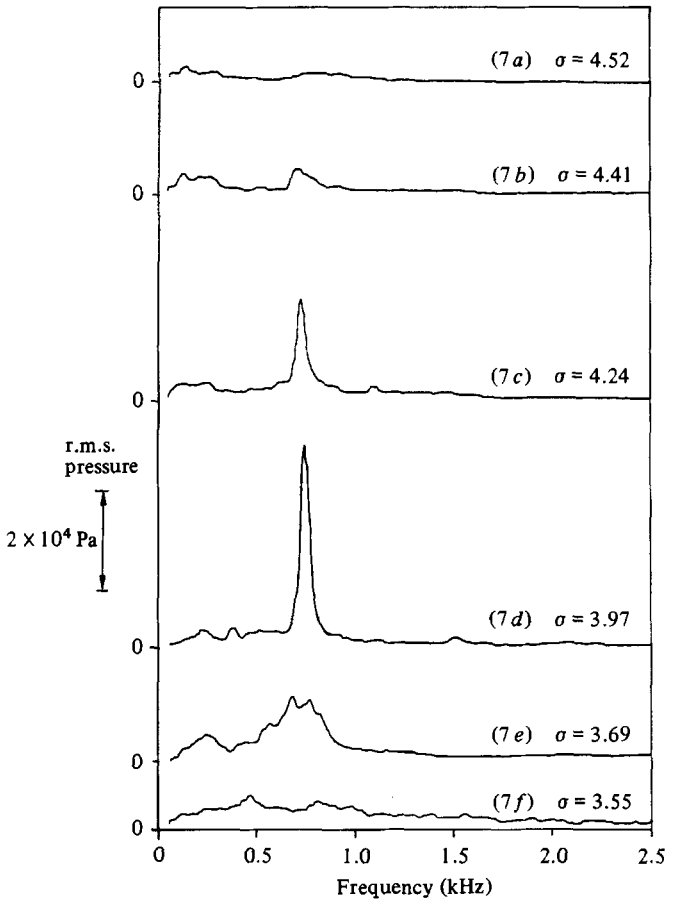

FIGURE 7. Noise spectra under different cavitation conditions; $U_\infty = 19$ m/s, $x = 200$ mm.

gives values of r.m.s. pressure and non-dimensional cavity length λ as a function of σ. It can be seen that peak noise occurs at $\sigma \approx 4$ when $\lambda \approx 2$. The experiments in §§4.1 and 4.2 were carried out under these flow conditions.

A description of the flow conditions that accompany changes in σ may be appropriate at this point.

4.3.1. *Flow observation*

On lowering σ cavitation started as a narrow band along the surface of the cylinder. This cavitation band lengthened in the streamwise direction with a further decrease in σ until it was terminating just downstream of the cylinder. At this point bubble cavitation started to develop about one diameter downstream of the cylinder centreline with the flow becoming markedly unsteady. The flow remained unsteady, causing the test section to vibrate, until cavitation was well established in this zone. Both the perceived noise in the laboratory and the r.m.s. pressure of the measured noise rose sharply with the onset of cavitation in the wake of the cylinder (see figure 6). The unsteadiness in the flow and the vibration of the test section reduced once the cavitation cloud became established downstream of the cylinder, but both the noise perceived in the laboratory and the measured noise continued to increase

as the cavitation zone grew on lowering σ. Both the noise in the laboratory and in the tunnel reach a peak when this cavitation zone appeared to be about two cylinder diameters in length. When σ was lowered further the noise reduced, but the flow again became unsteady causing vibration. This unsteadiness persisted until the cavity was five cylinder diameters in length. Thereafter the flow became steady and considerably quieter. Under these flow conditions the cavity appeared smooth and clear at its upstream end (near the cylinder), but frothy at its downstream end. Bubbles could be seen being swept downstream from the cavity termination.

4.3.2. *Noise spectra at different values of cavitation number*

The noise spectrum 200 mm downstream of the cylinder was measured at different values of σ. Figure 7 shows six such spectral curves. The values of σ at which these measurements were taken are given in figure 7 and are also indicated on the noise/cavitation-number characteristic in figure 6. It can be seen that the spectrum is nearly flat until cavitation starts in the wake when a peak develops in the spectrum at the shedding frequency. A narrow-band peak is readily identifiable when $\sigma = 4.24$. At this value of σ the cavitation cloud appeared as a short cavity of approximately one cylinder diameter in length. The noise spectrum shows that this cavitation cloud was not steady, but rather a time average of cyclic events with a well-defined period. Photographs of cyclic cavitation behind circular cylinders may be found in Varga & Sebestyen (1966*a*, *b*), Syamala Rao *et al.* (1972), Chandrasekhara & Syamala Rao (1973) and Syamala Rao & Chandrasekhara (1976).

The cavitation zone grows behind the cylinder as σ is lowered while the energy at the shedding frequency steadily increases i.e. the intensity of the cavity collapses increases. The peak in the noise spectrum reached its maximum amplitude at $\sigma = 3.97$. At lower values of σ this narrow-band noise collapsed rapidly into broad-band noise centred on the previously well-defined shedding frequency i.e. the cavity collapses were no longer accurately periodic, but had become more random. At even lower values of σ when a fixed (steady) cavity appeared the broad-band noise disappeared altogether, showing the cavity collapses were no longer regular.

5. Discussion

Before discussing the present results some consideration should be given to the Reynolds number at which these tests were carried out and to the considerable blockage of the test section (50 %). These effects are related since the flow conditions around the cylinder may not be characterized simply on Reynolds number calculated on upstream conditions in a tunnel with high blockage.

Roshko (1961) has shown that at Reynolds numbers greater than $R_e = U_\infty d/\nu = 10^3$ the flow around a circular cylinder (non-cavitating) of diameter d can be separated into four different regimes depending on boundary-layer separation conditions: subcritical, critical, supercritical and transcritical. In wind-tunnel tests Bearman (1969) obtained accurate measurements of the vortex-shedding frequency in the critical Reynolds-number-regime. Some of his measurements are reproduced in figure 8. It can be seen that the Strouhal number $S = fd/U_\infty$ increases from less than 0.2 in the subcritical flow regime to a value of 0.46 in the supercritical flow regime. After comparing his results with those of other investigators he concluded that the Strouhal number lies in the range $0.40 < S < 0.45$ in the supercritical flow regime. The value of $S = 0.4$ calculated here on the cavity-collapse frequency indicates that the present tests were conducted in the supercritical flow regime.

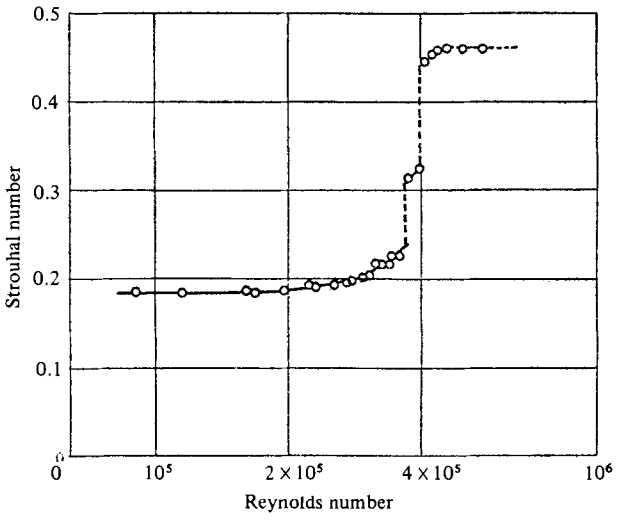

FIGURE 8. Variation of Strouhal number with Reynolds number. (From Bearman (1969).)

It is important to know the Reynolds-number regime in which tests are carried out since both the type of cavitation inception (Wykes 1979*a*) and the development of cavitation (Wykes 1979*b*) have been shown to depend on the noncavitating flow regime. Wykes (1979*a*) observed that cavitation inception appeared as a narrow band of bubbles on the surface of the cylinder along its span in the Reynolds-number range $2.3 \times 10^5 < R_e < 3.8 \times 10^5$. In this investigation ($R_e = 3.8 \times 10^5$ based on $U_\infty = 19$ m/s) this type of cavitation inception and the observed development of cavitation both indicate that tests were carried out in the supercritical flow regime.

It must be mentioned that measured cavity-collapse frequency appeared almost independent of σ in these tests (figure 7). This was also found by Selim (1981) using a geometrically similar tunnel. It is possible that the expected decrease in S was not observed because of the very high blockage in this tunnel. The cavity growth associated with a decrease in σ would increase the blockage further and this would increase the local velocity. The objective of the present work is to relate the cavity collapse intensity to the cavity development in the wake. The relationship between the cavity-collapse frequency and the cavitation number has already been investigated by Varga & Sebestyen (1966*b*), Syamala Rao *et al.* (1972), Syamala Rao & Chandrasekhara (1976) and Mussared (1978). It must be mentioned that the results of Syamala Rao & Chandrasekhara show a large variation from the results of the other investigators. Syamala Rao & Chandrasekhara found that the cavity-shedding frequency decreased as σ was lowered in reasonable agreement with the empirical curve given by Varga & Sebestyen until close to choking conditions. They then measured an increase in shedding frequency not measured by other investigators. Mussared suggested that this could be attributed to the high blockage (up to 25 %) in their tunnel. A different explanation is suggested here in terms of cavity structure. First, it should be noted that in the tests carried out by Varga & Sebestyen the cavitation number was only lowered to $\sigma = 1.5$, corresponding to a cavity of $\lambda \approx 2.5$, i.e. the tests were carried out on short cavity lengths where the cavity shedding was cyclic. Mussared carried out experiments over a wider range of σ, measuring the cylinder's response to vortex shedding by attaching a strain gauge to the cylinder. He found that the flow became steady as choking conditions were approached (in

agreement with the noise-spectrum results presented here). It is suggested that the apparent increase in shedding frequency close to choking conditions reported by Syamala Rao & Chandrasekhara was due to measuring bubble clusters breaking away from the downstream end of a fixed (steady) cavity rather than measuring a true cavity cycle frequency. They measured shedding frequency from high-speed photographs of the flow rather than using vibration or pressure-sensing techniques, and noted that the determination of vortex shedding became difficult near choking conditions. Syamala Rao *et al.* (1972) show some photographs of the flow downstream of the 9.5 mm diameter cylinder that they tested. From these photos it is clear that a fixed cavity existed at the value of σ at which an increase in shedding frequency was reported.

5.1. *Description of cavity-development process*

The existence of two cavity types is not new. Varga & Sebestyen (1966*a*) reported that a fixed (steady-state) cavity was produced for $\lambda > 3$. More recently Chandrasekhara & Syamala Rao (1973) reported one type of cavity for $\lambda < 2.0$ and another for $\lambda > 4.5$. However, the cavity-growth process has not been related to the damage capacity of the flow. As σ is lowered the vortices shed from either side of the cylinder are made visible by the onset of cavitation. It is believed that cavities develop either in the cores of these vortices or in the shear layers around them. The exact mechanism of inception has not been established. These cavities are swept downstream into a higher pressure field where they collapse regularly producing the narrow-band peak in the noise spectrum. The cavities within these vortices grow as σ is lowered and collapse with increased intensity (as shown in figure 7). However, at some point these cavities become so large that they begin to interfere with each other and also the cavity-shedding process itself. This causes the cavity shedding to become irregular and the cavities to be of different sizes. This is substantiated by noise samples, which show that under these conditions the cavity collapses vary in both amplitude and frequency. The intensity of the cavity collapses is greatest (producing the maximum r.m.s. pressure noise and the maximum erosion rate) when the shed cavities are as large as possible without interfering with the regular cavity-shedding mechanism. It was found that cavity collapses started to become irregular (from noise spectrum results) as soon as σ was reduced below its peak noise value. Further lowering σ causes gross cavity interference as the cavities grow until they coalesce to form a single cavity fixed to the cylinder itself.

The cavity-development processes described above are summarized in figure 6. Cavitation may start on the surface of the cylinder (depending upon the Reynolds number regime) but there is not appreciable increase in the noise until cavitation starts in the wake and this marks the beginning of cyclic cavitation. The intensity of these cyclic collapses increases until peak noise conditions are reached. Peak noise conditions mark the start of a transition zone to fixed cavity conditions. From flow observations fixed cavity conditions were only properly established at $\lambda \approx 5$, although from figure 6 it can be seen that rapid cavity length growth associated with fixed cavities started at $\lambda \approx 3$.

It is argued that the intensity of cavity collapses downstream of a cylinder is directly dependent upon cavity/wake dynamics, and that these may be characterized by the non-dimensional cavity length λ itself, i.e. the cavity-flow changes that give rise to peak noise (or peak damage) are primarily dependent upon λ. For example, in Syamala Rao *et al.* (1972) six cylinders of different diameters were tested in the same tunnel and it was found that there was a rapid increase in cavity length for

each cylinder when $\lambda \approx 3.5$ despite varying blockage (9–25%). It is difficult to estimate λ accurately, but this value is close to the value of $\lambda \approx 3$ in the present tests. Similarly, peak intensity was found to occur at $\lambda \approx 2$ in this investigation while values of $\lambda \approx 1.5$ and $\lambda \approx 2.5$ are reported in Varga & Sebestyen (1972) and Syamala Rao *et al.* (1972) respectively.

The general conclusion of this work relating peak noise to the end of the cyclic cavity collapse process may be true for other bluff bodies exhibiting periodic wakes. Young & Holl (1966) have reported cyclic collapses behind symmetric wedges. Accordingly, some experiments (similar to those reported here) were carried out in a 60° symmetric wedge in the present tunnel. The above relationship between peak noise and cavity mechanics was found to exist for this body also.

6. Conclusions

Measurements of noise spectra downstream of a cavitating circular cylinder together with flow observation have enabled the cavity-growth process to be described. As σ is lowered the cavities grow within the shed vortices and the intensity of their collapses increases until peak noise conditions are reached (at $\lambda \approx 2$). On lowering σ further the cavities interfere with the shedding process causing it to become irregular with subsequent decrease in cavity collapse intensity. The shed cavities coalesce to form a fixed (steady) cavity which becomes fully established at about $\lambda \approx 5$.

Peak cavitation-collapse intensity which produces maximum noise and maximum erosion rate occurs at the end of the cyclic collapse process when the collapsing cavities are as large as possible without affecting the cyclic process. The cavitation-collapse intensity is directly dependent upon the cavity/wake dynamics, which may be characterized by λ.

This work was conducted in the Department of Mechanical Engineering at the University of Southampton. The author wishes to thank Professor S. P. Hutton for his encouragement throughout the investigation. The work was supported by Procurement Executive, Ministry of Defence, and the author is grateful to the Admiralty Marine Technology Establishment, AMTE (Holton Heath) for the use of their digital r.m.s. voltmeter.

REFERENCES

BEARMAN, P. W. 1969 On vortex shedding from a circular cylinder in the critical Reynolds number regime. *J. Fluid Mech.* **37**, 577–585.

CHANDRASEKHARA, D. V. & SYAMALA RAO, B. C. 1973 Effect of pressure on the length of cavity and cavitation damage behind circular cylinders in a venturi. *Trans. ASME* D: *J. Basic Engng* **95**, 1–9.

HUTTON, S. P. & FRY, S. A. 1983 Correlation of cavitation noise and erosion. In *Proc. 2nd Conf. Cavitation, Heriot-Watt University, Edinburgh, Sept. 1983.*

LOBO GUERRERO, J. 1974 A study of the damage capacity of some cavitating flows. Ph.D. thesis, Mechanical Engineering Department, Southampton University.

LUSH, P. A. 1975 Noise from cavitation in venturi-type sections. In *Proc. 5th Conf. Fluid Machinery, Budapest, 1975*, pp. 427–438.

MUSSARED, M. R. 1978 Cavitation on a two-dimensional circular cylinder, M.Sc. thesis, Department of Engineering Science, Oxford University.

RAMAMURTHY, A. S. & BHASKARAN, P. 1979 Velocity exponent for erosion and noise due to cavitation. *Trans. ASME* I: *J. Fluids Engng* **101**, 69–75.

ROSHKO, A. 1961 Experiments on the flow past a circular cylinder at very high Reynolds number. *J. Fluid Mech.* **10**, 345–356.

SELIM, S. M. A. 1981 Cavitation erosion in fluid flow. Ph.D. thesis, Department of Mechanical Engineering, Southampton University.

SYAMALA RAO, B. C. & CHANDRASEKHARA, D. V. 1976 Some characteristics of cavity flow past cylindrical inducers in a venturi. *Trans. ASME* I: *J. Fluids Engng* **98**, 461–468.

SYAMALA RAO, B. C., CHANDRASEKHARA, D. V. & SEETHARAMIAH, K. 1972 A high-speed photographic study of vortex shedding behind circular cylinders of cavitating flows. In *Proc. 2nd Intl JSME Symp. Fluid Machinery and Fluidics, Tokyo, Sept. 1972*, pp. 293–302.

VARGA, J. J. & SEBESTYEN, G. 1966*a* Experimental investigation of cavitation noise. *Houille Blanche* **8**, 905–910.

VARGA, J. J. & SEBESTYEN, G. 1966*b* Determination of the frequencies of wakes shedding from circular cylinders. *Acta Tech.* **53**, 91–108.

VARGA, J. J. & SEBESTYEN, G. 1972 Determination of hydrodynamic cavitation intensity by noise measurement. In *Proc. 2nd Intl JSME Symp. Fluid Machinery and Fluidics, Tokyo, Sept. 1972*, pp. 285–292.

WYKES, M. E. P. 1979*a* Cavitation inception on a two-dimensional circular cylinder. In *Proc. NEL Fluid Mech. Silver Jubilee Conf., Nov. 1979.*

WYKES, M. E. P. 1979*b* The development of cavitation on a circular cylinder. In *Proc. NEL Fluid Mech. Silver Jubilee Conf., Nov. 1979.*

YOUNG, S. G. & HOLL, J. W. 1966 Effects of cavitation on periodic wakes behind symmetric wedges. *Trans. ASME* D: *J. Basic Engng* **88**, 163–176.